International Soil and Water Conservation Research 9 (2021) 405–418

Contents lists available at ScienceDirect

International Soil and Water Conservation Research

journal homepage: www.elsevier.com/locate/iswcr

Original Research Article

Characteristics of unsaturated soil slope covered with capillary barrier system and deep-rooted grass under different rainfall patterns

Yangyang Li [a], Alfrendo Satyanaga [b], Harianto Rahardjo [c, *]

[a] School of Civil and Environmental Engineering, Nanyang Technological University, Block N1, 50 Nanyang Avenue, Singapore
[b] School of Engineering and Digital Sciences, Nazarbayev University, Kabanbay Batyr Ave. 53, Nur-Sultan, 010000, Kazakhstan
[c] School of Civil and Environmental Engineering, Nanyang Technological University, Block N1, #1B-36, 50 Nanyang Avenue, 639798, Singapore

ARTICLE INFO

Article history:
Received 23 July 2020
Received in revised form
9 December 2020
Accepted 17 March 2021
Available online 1 April 2021

Keywords:
Unsaturated
Slope stability
Unsaturated soil
CBS
Vetiver grass

ABSTRACT

Rainfall-induced slope failures commonly occur in residual soil slopes. Slope failures are triggered by the reduction in soil strength. This is attributed to the decrease in soil suction due to rainwater infiltration. Slope covers like capillary barrier system and vegetative cover are effective methods that can be used to prevent rainfall-induced slope failures. The capillary barrier system is able to limit the rainwater infiltration, and vegetation can contribute to the increase in soil strength. Vetiver grass is widely planted in tropical and subtropical areas of the world for soil and water conservation. This study investigates the characteristics of unsaturated soil slope covered with capillary barrier system and Vetiver grass in comparison with the original slope through numerical analyses and field measurements. The analyses were carried out under the advanced, normal, and delayed rainfall patterns. The results of the analyses indicated that the capillary barrier system played a more significant role than the Vetiver grass in maintaining slope stability, although both the capillary barrier system and Vetiver grass contributed to the slope stability. In addition, both numerical analyses and field measurements showed that under the delayed and normal rainfall patterns, when antecedent rainwater infiltration could increase the soil moisture, the capillary barrier system performed much better compared to Vetiver grass in maintaining soil matric suctions and slope stability.

1. Introduction

Climate change has been a worldwide concern, and it impacts many parts of the planet. Climate change is not limited to temperature but also precipitation. Rainfall-induced slope failures are commonly observed within unsaturated soils located in different geological settings such as pyroclastic deposits (Comegna et al., 2016; Forte et al., 2019; Pirone, 2015), extensively weathered residual soils (Rahardjo et al., 2013; Pradhan & Kim, 2015), and colluvial weathered deposits (Sorbino and Nicotera, 2013). A higher number of rainfall-induced slope failures could occur (Rahardjo et al., 2013; Zhang et al., 2019) as heavy rainfalls become more frequent (Meteorological Services Singapore, 2018). Slope fails as rainwater infiltrates into the residual soil slope and soil strength decreases due to a decrease in the matric suction within the unsaturated zone of residual soil slope (Oh & Lu, 2015; Xion et al., 2019). Rainfall-induced slope failures can cause significant damage to infrastructure or even loss of life. It is important to protect slopes with appropriate measures. Two possible preventive measures against rainfall-induced slope failures are related to slope stabilization using capillary barrier system and vegetations.

The capillary barrier system has been studied and widely used as an effective soil cover in reducing rainfall infiltration (Ross, 1990; Stormont, 1996). It comprises a fine-grained layer of non-cohesive soil overlying a coarse-grained layer of non-cohesive soil. As the capillary barrier system is generally unsaturated, the difference in permeability of the fine-grained layer and the coarse-grained layer limits the water movement downward into the slope (Yan et al., 2019). When rainfall occurs, infiltrated water will be held in the fine-grained layer by the capillary force and water will be drained laterally from the fine-grained layer if the fine-coarse interface is sloped. The water can also be removed by evapotranspiration from

* Corresponding author.
E-mail addresses: yangyang.li@ntu.edu.sg (Y. Li), alfrendo.satyanaga@nu.edu.kz (A. Satyanaga), chrahardjo@ntu.edu.sg (H. Rahardjo).
URL: http://www.ntu.edu.sg/cee/staff/infrastructure/academic/chrahardjo.asp

https://doi.org/10.1016/j.iswcr.2021.03.004

the fine-grained layer, though restricted by climate (Morris & Stormont, 1999). Breakthrough occurs when water percolates into the coarse-grained layer and fine-grained layer approaches saturation. The precipitation exceeds the total of evapotranspiration and lateral diversion, and the capillary barrier is not effective in this case (Stormont, 1996).

A lower-cost slope preventive measure is utilizing vegetation for covering the slope. Vegetation can affect slope stability by affecting soil hydrological and mechanical properties (Schwarz et al., 2010; Wang et al., 2019). Structural roots of trees and shrubs provide additional mechanical reinforcement to stabilize slopes significantly while fine roots of vegetations can help increase the shear strength of soil. Furthermore, rainwater could be intercepted by vegetation and soil water could be removed through the evapotranspiration process. These hydrological reinforcements result in a decrease in soil moisture and an increase in soil strength (Greenwood et al., 2004). However, many studies have shown that evapotranspiration was minimal and can be ignored during rainfall events (Leung et al., 2015; Ni et al., 2018). Compared to the effect of evapotranspiration, the root-induced changes in soil-water characteristic curve (SWCC) affected slope stability more than other factors (Ni et al., 2018). However, the effect of root-induced change in SWCC was not as significant as the effect of root-induced change in soil saturated permeability on slope stability (Leung et al., 2015). The hydrological reinforcement was predominantly contributed by the change in the saturated permeability. It was found that shallow soil was effectively reinforced by the mechanical effect of roots while deep soil was more reinforced by the hydrological effects of roots (Ni et al., 2018). In addition, soil permeability could increase due to the root channels formed by the macropores that were created by dying and decaying roots, which could endanger slope stability (Ni et al., 2018). On the other hand, Ghestem et al. (2011) suggested that both alive and dead roots can form preferential flow paths, and the effects can be adverse or beneficial to slope stability depending on the root arrangement and architecture in the slope.

Both capillary barrier system (CBS) and vegetations help to stabilize the slope. However, the comparison of the effectiveness of both methods on stabilizing an unsaturated soil slope was seldom studied. Furthermore, slopes may also behave differently under different rainfall patterns such as advanced rainfall, normal rainfall, and delayed rainfall (Rahimi et al., 2011). Ng et al. (2001) found that rainfall patterns influenced the pore-water pressure changes significantly, although the resultant change in slope stability was not investigated. Rahimi et al. (2011) studied the effect of three typical rainfall patterns on slopes with two different soil types (with high and low permeability) and found that the slope stability of low permeability soil slope was affected more than the slope stability of high permeability soil slope by the rainfall patterns. Brand et al. (1984) also suggested that landslides in Hong Kong were mostly induced by rainfall with short duration and high intensity. In addition, the effect of antecedent rainfall was very limited due to the high permeability of local soils in Hong Kong.

Issues related to runoff and soil erosion due to rainfall have been extensively studied by Cuomo et al. (2015; 2016a; 2016b) in different scales. In our case, soil erosion due to runoff was not considered because Singapore is an urbanized city with very good drainage systems. Soils in Singapore are relatively stiff and not much erosive. Most slopes are engineered slopes and the soil was well compacted. In addition, our cumulative precipitation applied in this study was less than 400 mm and runoff can hardly occur, based on a study by Cuomo and Della Sala (2013) for slopes under rainfall intensity higher than the initial hydraulic soil permeability but lower than the saturated permeability.

In this study, the characteristics of three different slopes, i.e., one original residual soil slope, one residual soil slope covered with CBS, and another residual soil slope covered with deep-rooted Vetiver grass were investigated. The main objective of this study is to compare the characteristics of these three different slopes under the advanced, normal, and delayed rainfall patterns. The effectiveness of the two different slope stabilization methods under different rainfall patterns were compared through parametric studies and field measurements. The parametric studies were conducted numerically on the performance of different slopes under different rainfall patterns. On the other hand, field monitoring measurements of soil suctions at different depths were used to evaluate the characteristics of different slopes under different rainfall patterns.

2. Method of analyses

2.1. Rainfall patterns in parametric studies

Parametric studies were carried out numerically to investigate the performance of three slopes under three rainfall patterns. Seepage analyses were conducted first using SEEP/W (Geo-slope international Ltd, 2012a; Geo-slope international Ltd, 2012b) to obtain the pore-water pressure changes due to rainwater infiltration, to be exported to SLOPE/W (Geo-slope international Ltd, 2012a; Geo-slope international Ltd, 2012b) for calculation of factor of safety (FOS). The three slopes investigated in this study comprised original residual soil slope, residual soil slope covered with CBS, and residual soil slope covered with Vetiver grass. The three rainfall patterns applied in the transient seepage analyses were advanced rainfall, normal rainfall, and delayed rainfall following the study by Rahimi et al. (2011). According to a study by Rahardjo et al. (2008), the highest pore-water pressure profile was observed when a total of 5-day antecedent rainfall was received by the slope, and the contribution of the subsequent rainfall to the pore-water pressure was insignificant. It was also found that a 5-day antecedent rainfall of 92–109 mm was the threshold to produce the highest pore-water pressure profiles in the residual soil derived from Bukit Timah Granite. Therefore, a 5-day rainfall of 100 mm was used in the simulation because it resulted in the highest pore-water pressure profile and the most unfavourable condition for slope stability. To distinguish the different antecedent rainfall patterns, the 5-day rainfall was divided into 15 time-intervals with 8 h duration for each time interval. The three rainfall patterns are shown in Fig. 1.

2.2. Site overview and soil properties

A slope investigated in this study is located at Ang Mo Kio St. 21 in Singapore. The slope consists of the residual soil from Bukit Timah granite. The slope was repaired upon major failures triggered by rainfall in 2008. The height and the slope angle of the repaired slope were 5 m and 33° respectively. One section of the slope was covered with CBS and another section of the slope was covered with Vetiver grass, as shown in Fig. 2. Each section of the slope had a total area of approximately 140 m^2. In the construction of CBS, granite chip was used as the coarse-grained material and fine sand was used as the fine-grained material. Each layer of the CBS system had a thickness of 20 cm. A related study about the performance of the same CBS slope through field instrumentations was discussed by Rahardjo et al. (2012). The vegetated slope was assumed to have a root depth of 40 cm for an estimation of short-term slope stability after planting Vetiver grass.

The undisturbed soil samples were taken using a Mazier sampler in the field. For the vegetated slope, the grass above the ground surface was removed first, and topsoil with roots was

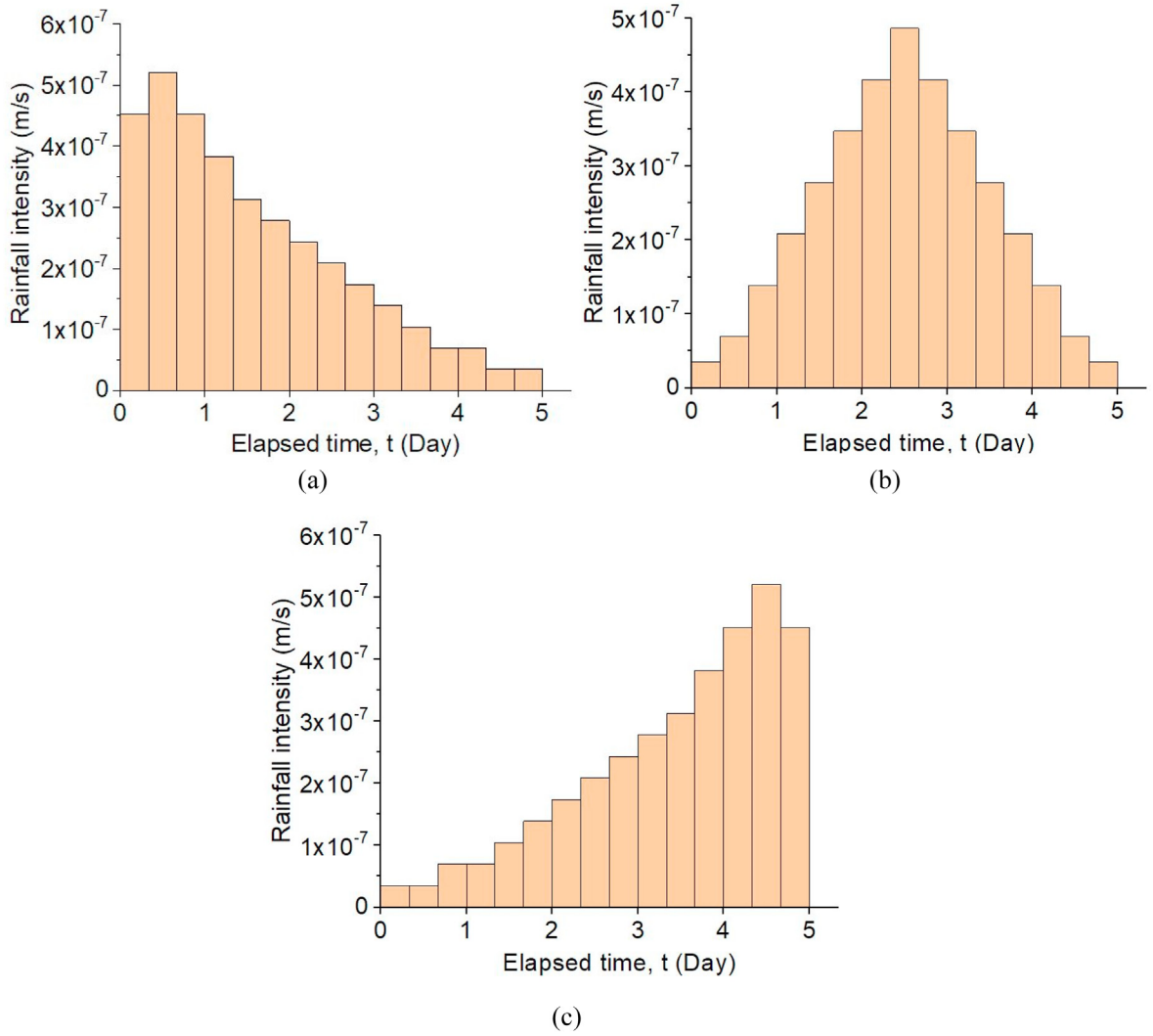

Fig. 1. The (a) advanced rainfall pattern, (b) normal rainfall pattern and (c) delayed rainfall pattern.

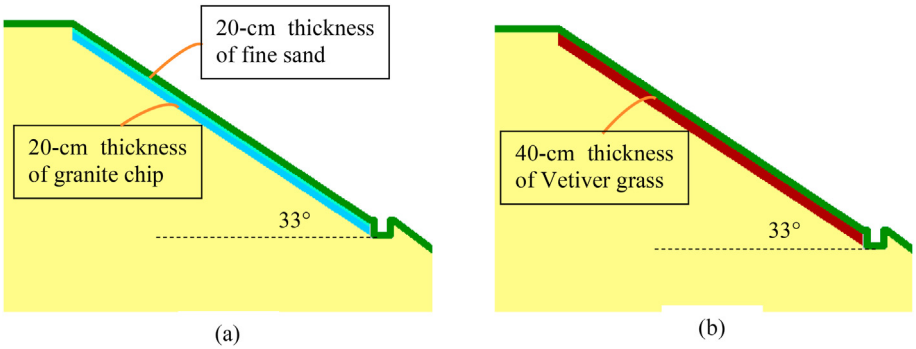

Fig. 2. (a) Slope covered with CBS and (b) slope cover with Vetiver grass.

sampled directly below the ground surface using block sampling. Index property tests, saturated permeability tests, and shear strength tests were carried out on those undisturbed samples in the laboratory. The saturated permeability tests were conducted using two back pressures triaxial system (Satyanaga et al., 2019). A summary of the basic properties of the soil used in this study is presented in Table 1.

The soil-water characteristic curve (SWCC) describes the relationship between the volumetric water content and matric suction of a soil. The air-entry value is the matric suction value when air starts to enter the pores during drying process and the water-entry value is the matric suction value when water starts to enter the pores during wetting process. The water-entry value is also called as the breakthrough head or breakthrough suction because

Table 1
List of soil index properties.

Index Properties	Residual soil	Fine sand	Granite chip	Topsoil with Vetiver grass
Unified soil classification system	SM-MH	SP	GP	SP
Specific gravity	2.64–2.68	2.65	2.69	2.64
Liquid limit (%)	53–66			
Plastic limit (%)	36–38			
Water content (%)	46–54			17.2
D_{60} (mm)	0.25	0.6	18	1.1
D_{30} (mm)	0.02	0.4	15	0.5
D_{10} (mm)	0.00	0.3	11.27	0.23
Coefficient of uniformity	92.86	2	1.6	4.89
Coefficient of curvature	0.63	0.89	1.11	1.01
Gravel (>4.75 mm; %)	0	5.4	98.5	11.9
Sand (%)	54	94.3	1.48	85.7
Fines (<0.075 mm; %)	46	0.3	0.002	2.4
Dry density (Mg/m^3)	1.51	1.56	1.65	1.86
Void ratio	0.74–0.77	0.70	0.64	0.4
Saturated coefficient of permeability (m/s)	6×10^{-6}	2.7×10^{-4}	5.1×10^{-1}	2.6×10^{-5}

breakthrough occurs when the matric suction at the interface between the fine-grained layer and coarse-grained layer is lower than the water-entry suction of the coarse-grained layer. Breakthrough occurs faster and easier when the water-entry value of the coarse-grained layer is higher. The SWCCs were best fitted using Fredlund and Xing (1994) Equation, which was found to fit data ranging from 0 to 1,000,000 kPa:

$$\theta = C(\psi)\frac{\theta_s}{\left\{\ln\left[e + \left(\frac{\psi}{a}\right)^n\right]\right\}^m} \quad (1)$$

where θ is the calculated volumetric water content for a specified matric suction; θ_s is the saturated volumetric water content; $C(\psi)$ is the correction factor and was suggested to be equal to 1 by Leong and Rahardjo (1997); ψ is the matric suction; and a, n, and m are empirically-derived variables related to the air-entry value of soil, the maximum slope of the SWCC and the curvature of the slope of SWCC, respectively.

Unsaturated permeability is determined from the measured saturated permeability and the integration of the SWCC (Fredlund et al., 1994; Zhai & Rahardjo, 2015):

$$k_w(\psi) = \frac{\int_{\ln(\psi)}^{b} \frac{\theta(e^y) - \theta(\psi)}{e^y}\theta'(e^y)dy}{\int_{\ln(\psi_{aev})}^{b} \frac{\theta(e^y) - \theta_s}{e^y}\theta'(e^y)dy}k_s \quad (2)$$

where b is equal to ln (100000); $k_w(\psi)$ is the calculated unsaturated permeability for a specified matric suction ψ (m/s); k_s is the coefficient of saturated permeability and y is a dummy variable of integration representing the logarithm of matric suction.

Tempe cell and pressure plates were the two instruments used to obtain SWCC data points. Fig. 3 shows the wetting SWCCs and permeability functions calculated from the measured saturated permeability and SWCC for the residual soil, fine sand, granite chips, and topsoil with Vetiver grass. The best-fitting parameters are summarized in Table 2. A simple scaling method proposed by Pham et al. (2005) was used for estimating the wetting curve for the granite chip in the coarse-grained layer.

Shear strength of unsaturated soils can be obtained using Equation (3), as proposed by Fredlund et al. (1978):

$$\tau = c' + (\sigma - u_a)\tan\varphi' + (u_a - u_w)\tan\varphi^b \quad (3)$$

where c' is the effective cohesion, φ' is the frictional angle, u_a is the pore-air pressure; $(\sigma - u_a)$ is the net normal stress; $(u_a - u_w)$ is matric suction and φ^b is the angle indicating the rate of change in shear strength with respect to the change in matric suction.

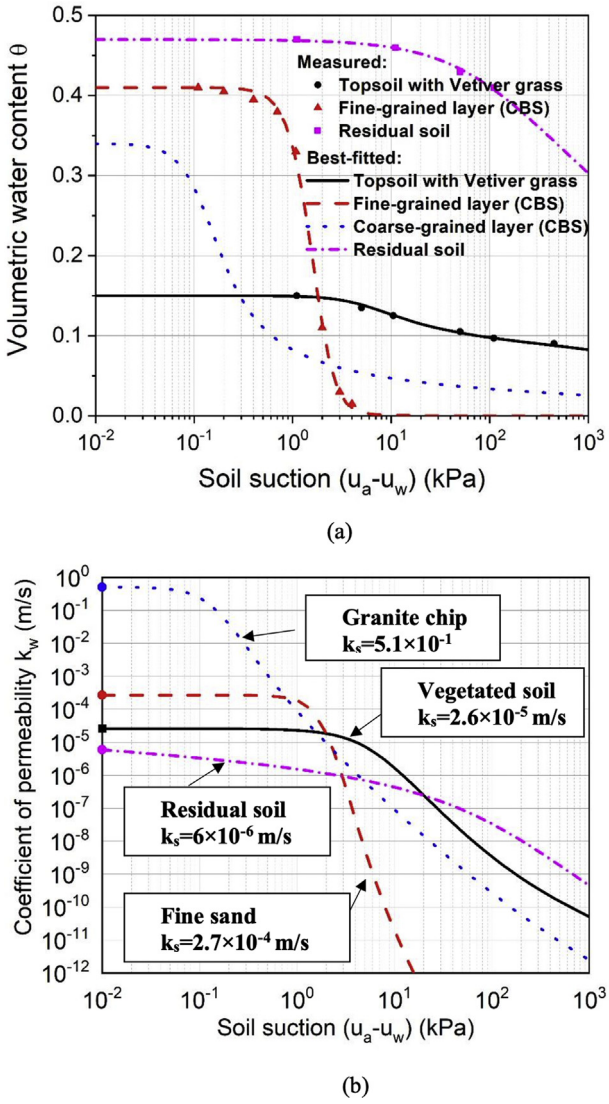

Fig. 3. (a) SWCCs and (b) permeability functions of the soils.

Table 2
Best-fitting parameters for the SWCCs.

Parameters	Residual soil	Fine sand	Granite chip	Topsoil with Vetiver grass
Saturated volumetric water content θ_s	0.47	0.41	0.34	0.15
a (kPa)	84.39	1.81	0.11	4.31
n	0.92	3.19	2.72	2
m	0.42	3.74	0.79	0.23

Multistage consolidated drained triaxial tests were carried out to obtain the shear strength parameters. Triaxial tests were conducted on the saturated soil specimens to obtain φ' and c'. Triaxial tests were conducted on the unsaturated soil specimens under a constant net normal stress but different matric suctions to estimate φ^b. More related details can be referred to the studies by Rahardjo et al. (2014) and Satyanaga et al. (2019). The shear strength parameters of the soils used in this study are shown in Table 3.

As illustrated in Fig. 4 and Fig. 5, steel J-pins of 1.5 m length were used to secure the CBS onto the slope. Each J-pin has a pull-out resistance of 10 kPa and a shear force of 15 kN.

2.3. Seepage and slope stability analyses in parametric studies

Seepage analyses were carried out to obtain the pore-water pressure changes due to different rainfall patterns. The initial ground water table was set to estimate the initial pore-water pressure head and the corresponding volumetric water content in the numerical analyses. The initial groundwater table was assumed the same for all three slopes. Fig. 6 illustrates the boundary conditions applied in SEEP/W. Unit flux was applied to simulate rainfall on the ground surface. No ponding selection was enabled by limiting the resultant maximum pore-water pressure to zero. Runoff was allowed and excess accumulation of rainwater on slope surface could be avoided. The total head of left boundary and right boundary were kept constant at 116.5 m and 115 m according to the position of groundwater table on site, respectively. At the bottom boundary, no flow was allowed. In addition, as illustrated in Fig. 6, a horizontal drain was installed to draw down the water level and reduce the excess pore water pressure in the slope.

At the end of each time interval (8 h), the factor of safety (FOS) was computed using Slope/W based on the pore-water pressures obtained from the previous seepage analysis for each slope. Bishop's simplified method of slices (Bishop, 1955) was used.

2.4. Field instrumentations and slope stability analyses

Three sections of the slope at Ang Mo Kio were instrumented with jet fill tensiometers for measurements of the negative pore-water pressure within the original slope, slope covered with CBS, and slope covered with Vetiver grass. The tensiometers were installed in mid-slope at depths of 0.5 m, 1 m, 1.5 m and 2 m with a spacing of 0.5 m. Maintenance was performed regularly to remove accumulated air resulted from cavitation of water by flushing the tensiometers and refilling deaired water into the jet-fill reservoir. Three piezometers were installed at the crest, middle and toe of the slope to monitor the position of groundwater table during dry and rainy periods. From September 2008 to October 2008, manual monitoring and maintenance of tensiometers were conducted three times a week at the same time of each day. The rainfall data were obtained from the nearest weather station, Ang Mo Kio weather station which was located 0.9 km distance away from the investigated site (i.e., Ang Mo Kio St. 21). Soil properties from the site as presented in Section 2.2 were incorporated in the numerical analyses of field instrumentation data.

Slope stability analyses were performed by incorporating the measured matric suction values from field monitoring in Slope/W using the total cohesion method (Fredlund & Rahardjo, 1993). The soil model was divided into five sublayers based on the following depths: 0–0.75 m, 0.75–1.25 m, 1.25–1.75 m, 1.75–2.25 m and the soil layer below 2.25 m. Based on the extended Mohr-Coulomb yield criterion for unsaturated soil (Fredlund et al., 1978) (i.e., $\tau = c' + (\sigma - u_a)\tan\varphi' + (u_a - u_w)\tan\varphi^b$), total cohesion c was defined as the summation of effective cohesion c' and additional cohesion from matric suction in unsaturated soil $(u_a - u_w)\tan\varphi^b$ (i.e. $c = c' + (u_a - u_w)\tan\varphi^b$). Total cohesions within the four soil layers close to the ground surface were calculated from the matric suctions observed from the field monitoring in each corresponding layer. A higher or lower matric suction reflected by the effect of rainwater infiltration resulted in a higher or lower additional cohesion from matric suction. The total cohesion was assumed constant and not to vary with depth within each layer.

Total cohesion method was used for the calculation of shear strength of the soil layers shallower than 2.25 m. For the soil deeper than 2.25 m without matric suction measurements, the soil shear strength was estimated based on the position of the ground water table as measured in the field. The extended Mohr-Coulomb yield criterion for unsaturated soil was applied with the shear strength parameters as listed in Table 3. The variations in matric suctions with depth were obtained based on the position of the groundwater table from the field measurements. It was assumed that all the three slopes shared the same groundwater table as measured in the field. In other words, the effect of Vetiver grass and CBS on groundwater level was not considered.

3. Results and discussions

3.1. Slope stability from parametric studies

Fig. 7 presents the results of stability analyses under three typical rainfall patterns (i.e., advanced rainfall pattern, normal rainfall pattern. and delayed rainfall pattern) from parametric

Table 3
Shear strength parameters of the soils.

Parameters	Residual soil	Fine sand	Granite chip	Topsoil with Vetiver grass
Unit weight γ (kN/m^3)	20	24	24	21.4
c′ (kPa)	2	0	0	10
φ' (°)	30	34	36	34
$\varphi^{\mathbf{b}}$(°)	18	15	17	19

Fig. 4. J-pins before (a) and after (b) installation.

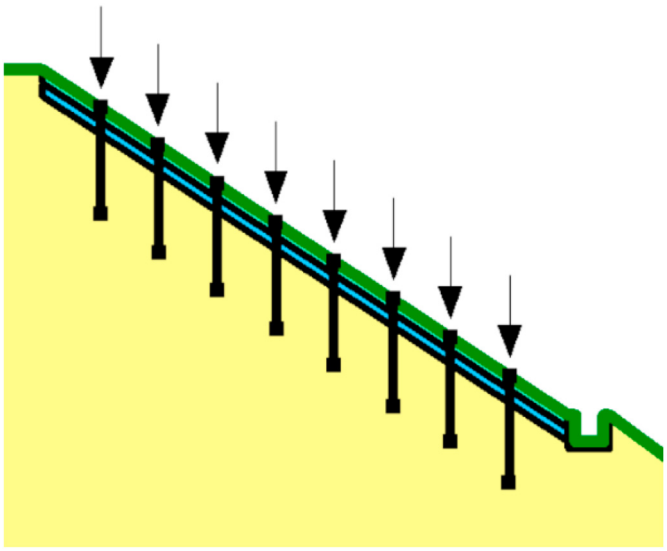

Fig. 5. Illustration of J-pins on slope covered with CBS.

studies, respectively. CBS, VG and OS represent the results of the CBS slope, the vegetated slope, and the original slope, respectively. The difference in the FOS of the CBS slope and the original slope, as well as the difference in the FOS of the vegetated slope and the original slope were plotted for comparison.

In general, the FOS of the CBS slope and the vegetated slope were higher than that of the original slope, which implied that both CBS and vegetations help to stabilize the slope. However, the FOS of the CBS slope was much higher than those of vegetated slope. Based on the analyses under the advanced rainfall pattern, the FOS of the CBS slope was about 15–20% higher than those of original slope, while the FOS of the vegetated slope was only about 2.5% higher than those of the original slope. Based on the analyses under the normal rainfall pattern, the FOS of the CBS slope was about 14–25% higher than those of the original slope, while the FOS of the vegetated slope was only about 2–4% higher than those of the original slope. Based on the analyses under the delayed rainfall pattern, the FOS of the CBS slope was about 17–25% higher than the FOS of the original slope, while the FOS of the vegetated slope was only about 2.5% higher than those of the original slope. The results of the slope stability analyses under different rainfall patterns

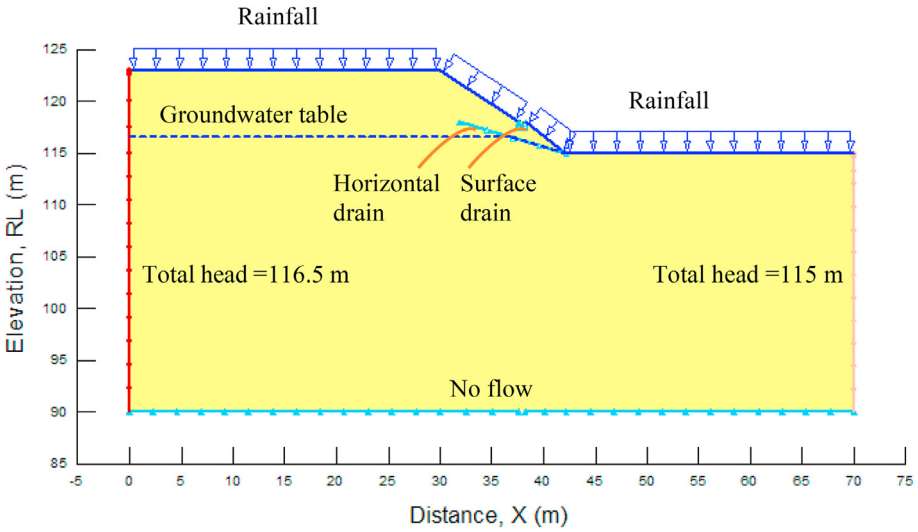

Fig. 6. Boundary conditions applied in seepage analyses.

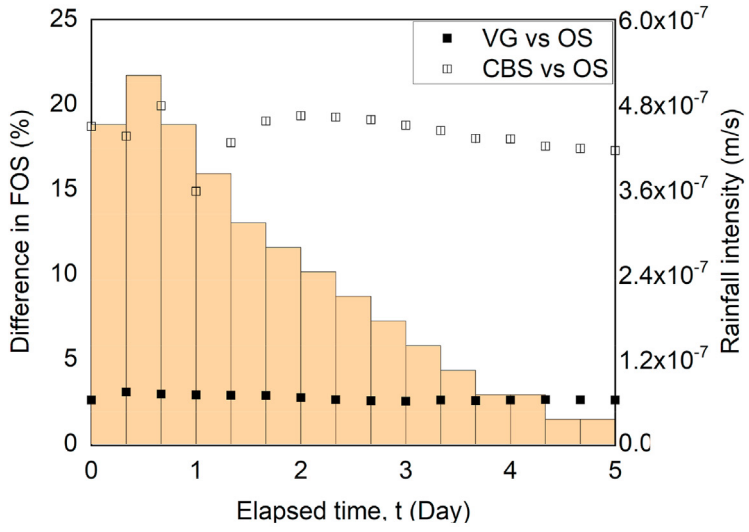

Fig. 7. The results of difference in the FOS of the vegetated slope, CBS slope and original slope under the (a) advanced rainfall pattern, (b) normal rainfall pattern and (c) delayed rainfall pattern.

indicated that the stability of the CBS slope might experience a significant drop during the application of rainfall with high intensity, as a result of the breakthrough. Breakthrough was observed from the results of seepage analyses on days with a high rainfall intensity. As the infiltrated rainwater within the fine-grained layer was diverted down to the lower part of the slope, breakthrough first occurred at the toe of the covered slope and in the end, it occurred at the top of the covered slope. Breakthrough was a progressive process under the prolonged light rainfall condition. However, under the short-duration heavy rainfall, breakthrough occurred at the same time along the slope because the infiltration rate was larger than the diversion capacity and the infiltrated water was not able to flow downwards before breakthrough occurred (Li et al., 2013). Significant infiltration into the underlying residual soil after breakthrough at a certain location lowered the FOS of the CBS slope. The distance from the top of the covered slope to the breakthrough position is called diversion length. Under the advanced rainfall pattern, breakthrough started immediately from the beginning of precipitation and reached a minimum diversion length of 3 m at the end of the first day. The FOS also reached the minimum value at the same time. Under the normal rainfall pattern, breakthrough started from the morning of the 2nd day and the FOS started to decrease. The minimum diversion length was about 6 m at the end of the third day. The minimum FOS also occurred at the same time. Under the delayed rainfall pattern, breakthrough started from the 4th day of precipitation and reached a minimum diversion length of 3 m at the end of the 5th day. The FOS also reached minimum at the same time. It was found that the minimum FOS occurred at the same time when the diversion length reached the minimum in all three analyses under different rainfall patterns. Moreover, a shorter diversion length resulted in a lower FOS. It was also observed that the stability of the CBS slope was more sensitive to the change in rainfall patterns, as a result of breakthrough, compared to the stability of the original slope and the vegetated slope.

In the parametric studies, the contribution of the Vetiver grass on the evapotranspiration was ignored and this may cause an underestimate of the computed FOS values of the vegetated slope.

3.2. Field measurements

Variations in groundwater level with the daily precipitation in September and October 2008 at Ang Mo Kio slope are presented in Fig. 8. As observed, the groundwater level at the toe of the slope was maintained at the ground surface due to the presence of the horizontal drain.

Figs. 9–11 show the field measurements of matric suctions at various depths for the original slope, vegetated slope and CBS slope in September and October 2008. The daily precipitation data from the nearest weather station located 0.9 km away was also plotted.

It was observed that the matric suction values from field monitoring of the CBS slope were generally higher than those measured in the vegetated slope and original slope, which contributed to the additional shear strength of soil at the CBS slope. In addition, the J-pins installed in the CBS slope also contributed partly to the stability of the slope. Hence, the stability of a CBS slope can be maintained during rainfall. The highest daily precipitation of 100 mm was recorded on September 3 that resulted in a significant drop in matric suctions of all three slopes. The range of the matric suction from field monitoring of the CBS slope varied from 2.5 to 20 kPa while those of the vegetated slope and original slope varied from 0 to 11 kPa and from 0 to 6 kPa, respectively. Furthermore, there was a relatively high daily precipitation of 44 mm on September 26. However, the matric suction of the CBS slope was maintained between 20 and 40 kPa varying with depth while the matric suction of the vegetated slope and original slope dropped to a range between 2 and 18 kPa and between 7 and 9 kPa, respectively. It implied that the stability of the CBS slope might not be affected by rainwater since CBS impeded the rainwater infiltration while the vegetated slope and original slope were much more affected by the rainwater infiltration. In October 2008, although the daily precipitation was not higher than 22 mm, there was a long period of continuous precipitation from October 13 to October 22. Due to this long period of rainfall, the matric suction of all three slopes dropped significantly. However, CBS was still effective as a slope cover since it can maintain a relatively higher matric suction.

In both September and October, the matric suction values from field measurements of the vegetated slope at 0.5 m and 1 m depth were the lowest among all slopes. However, the matric suction values at 1.5 m of the vegetated slope were much higher than that of the original slope, which can be observed clearly from the plots of matric suctions for all slopes with respect to different depths as shown in Figs. 12–15. The shallow layer (i.e., 0-1 m) of the vegetated slope may have a higher storage of water due to the existence of vegetations. Matric suction decreased more significantly within the shallow soil layer instead of the deeper soil layer, implying lesser rainwater infiltration into the deeper soil layer below 1 m. The high suction of the vegetated slope at 1.5 m depth was also contributed by a concentration of roots above the depth. However, the soil suction at 2 m depth was not as high as the soil suction at 1.5 m because 2 m depth was close to the groundwater table (i.e., 2-5 m between middle and crest of slope). The observed low suctions at shallow soil (i.e., 0-1 m) and high suctions at deep soil (i.e., 1.5 m) of the vegetated slope implied the same conclusion from the study by Ni et al. (2018) that the shallow soil (i.e., 0-1 m) was more reinforced by the mechanical effect of roots while deep soil (i.e., 1-2 m) was more reinforced by the hydrological effects of roots.

It was also observed that the rainwater infiltration into the layer below the CBS slope was reduced. As a result, the matric suction within the layer near the ground surface of the CBS slope was also maintained at a higher suction value as compared to that of the vegetated slope and original slope. This could be attributed to the lateral diversion of rainwater within the fine-grained layer of the CBS slope. Then, the rainwater was dissipated into the main drain further downslope. Therefore, the difference in the matric suction between field measurements from the CBS slope and the original slope was observed to be small at 0.5 m depth since the infiltrated rainwater flowed within the fine-grained layer. On the other hand, the difference in the matric suction between field measurements from the CBS slope and the original slope was observed to be large at the deeper soil layer since only limited rainwater was able to infiltrate into the soil layer below CBS.

3.3. Slope stability from field measurements

Slope stability analyses that incorporates the field measurements of matric suctions and groundwater table were then performed in Slope/W using total cohesion method. The periods of field measurements to be incorporated in the slope stability analyses were selected based on a period with similar rainfall patterns as used in the parametric studies. Fig. 16 presents the computed FOS based on the analyses under the advanced, normal and delayed rainfall patterns. Meanwhile, the difference in the FOS from analyses of the CBS slope and the original slope, as well as the difference in the FOS from the analyses of the vegetated slope and the original slope was calculated and plotted.

In general, both CBS and vegetations helped to stabilize the slope as the FOS of the CBS slope and the vegetated slope were higher than that of the original slope. However, CBS performed better in maintaining the slope stability since the FOS of the CBS

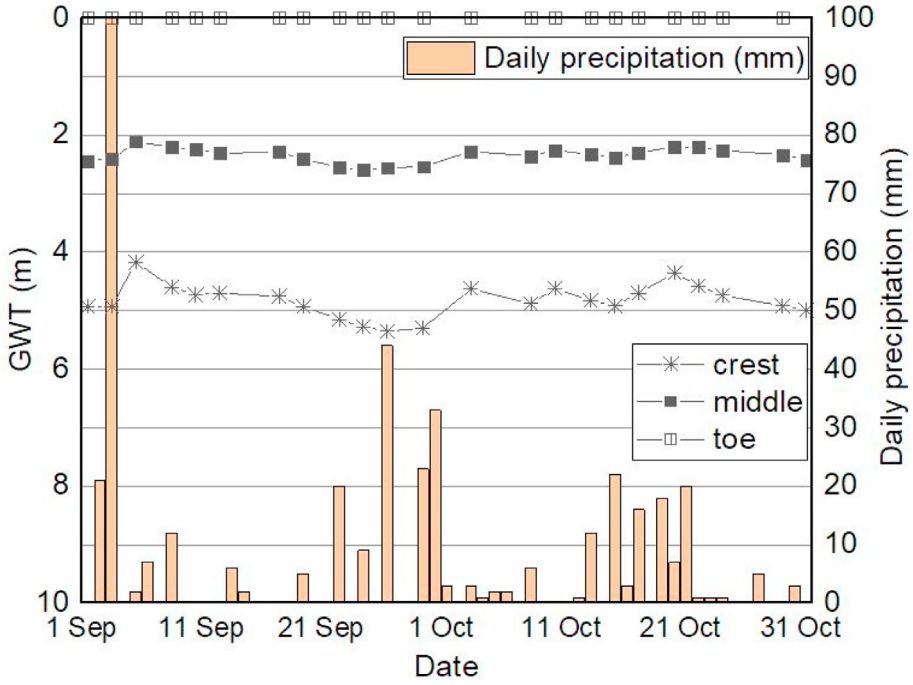

Fig. 8. Piezometer measurements at the crest, middle and toe of slope.

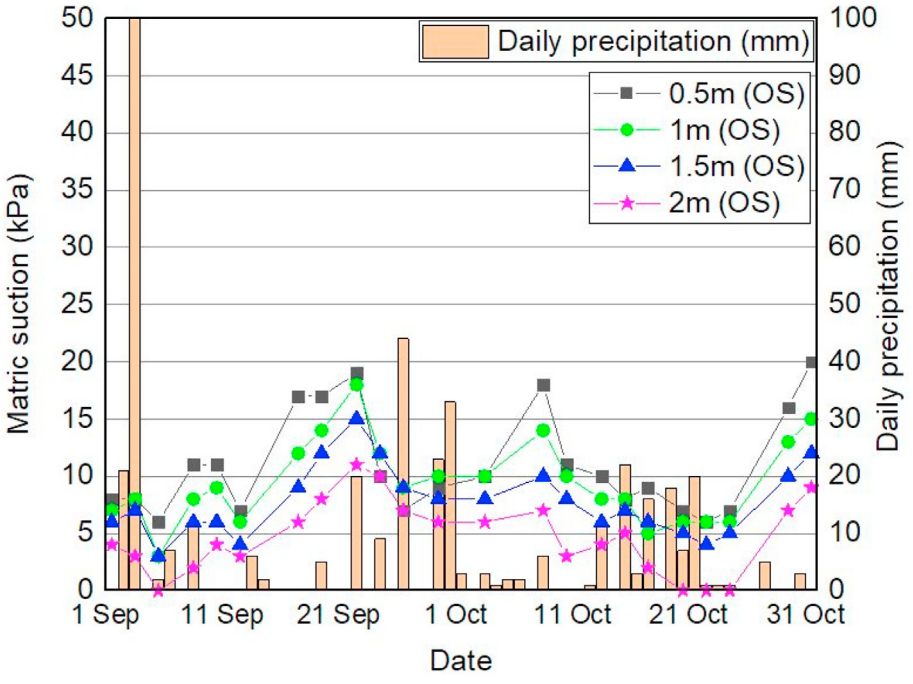

Fig. 9. Tensiometer measurements at various depths for the original slope.

slope was higher than that of the vegetated slope. The minimum FOS for the CBS slope was 1.4, 1.5 and 1.6 based on the stability analyses under the advanced, normal and delayed rainfall patterns, respectively. The minimum FOS for the vegetated slope were 1.4 based on the stability analyses under the advanced and normal rainfall patterns and 1.5 based on the stability analyses under the delayed rainfall pattern. The minimum FOS for the original slope were 1.3 based on the stability analyses under the advanced and normal rainfall patterns and 1.5 based on the stability analyses under the delayed rainfall pattern. The analyses on certain rainy days (i.e., Sep 26 and Oct 22) indicated that the FOS of the CBS slope did not decrease with the help of the capillary layer to minimize the rainwater infiltration, while those of the vegetated slope and the original slope decreased.

Based on the stability analyses under the advanced rainfall pattern, the FOS of the CBS slope was about 4–11% higher than the FOS of the original slope, while the FOS of the vegetated slope was about 1.5–8% higher than the FOS of the original slope. Based on the stability analyses under the normal rainfall pattern, the FOS of the CBS slope was about 6–12% higher than those of the original

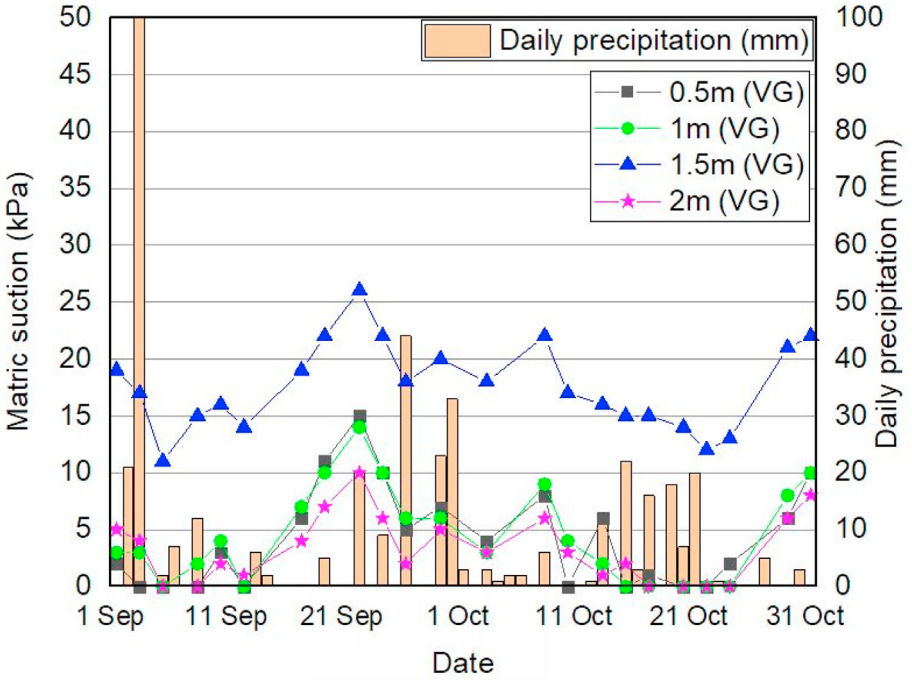

Fig. 10. Tensiometer measurements at various depths for the vegetated slope.

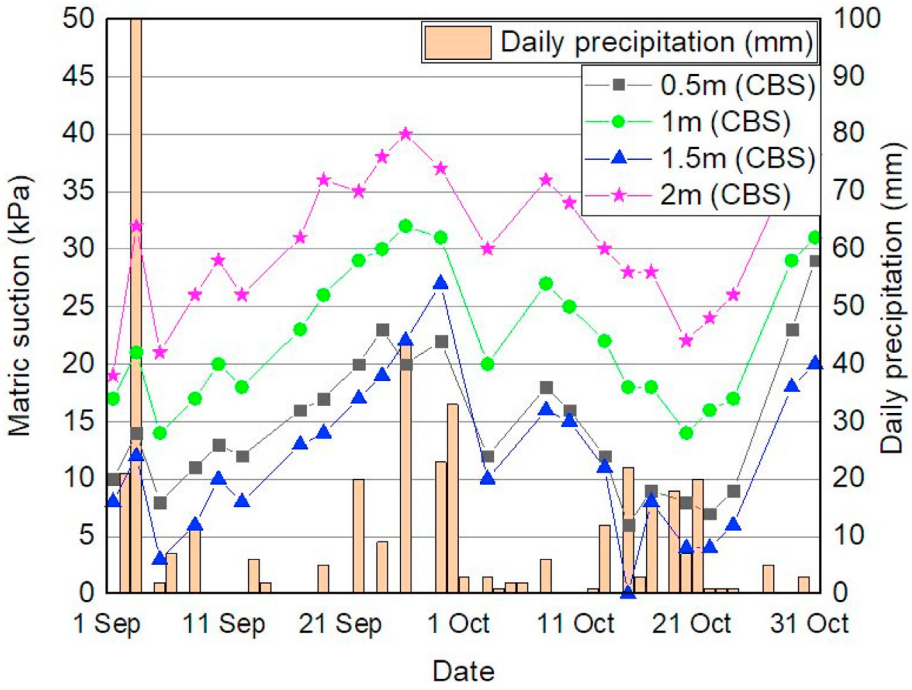

Fig. 11. Tensiometer measurements at various depths for the CBS slope.

slope, while the FOS of the vegetated slope was about 3–7% higher than those of the original slope. Based on the stability analyses under the delayed rainfall pattern, the FOS of the CBS slope was about 2.5–7% higher than those of the original slope, while the FOS of the vegetated slope was about 1.5–2% higher than those of the original slope.

In Table 4, the effectiveness of CBS and Vetiver grass in slope stability under different rainfall patterns were compared by summarizing the difference in the FOS from both parametric studies and field measurements. CBS performed better when compared to Vetiver grass in maintaining slope stability under the delayed and normal rainfall patterns than under the advanced rainfall pattern, implying that the antecedent rainwater infiltration under the delayed and normal rainfall patterns could affect the vegetated and original slopes more than the CBS slope.

It was also observed that the differences in the effectiveness of CBS and Vetiver grass observed from the analyses incorporating field measurements were not as large as observed from the

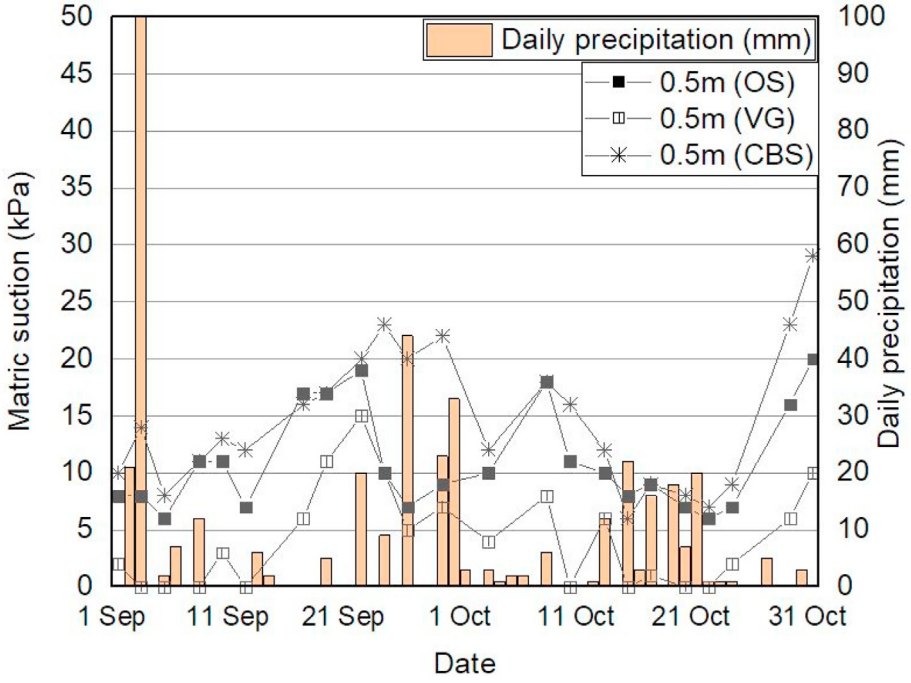

Fig. 12. Tensiometer measurements at 0.5 m for the original slope, vegetated slope and CBS slope.

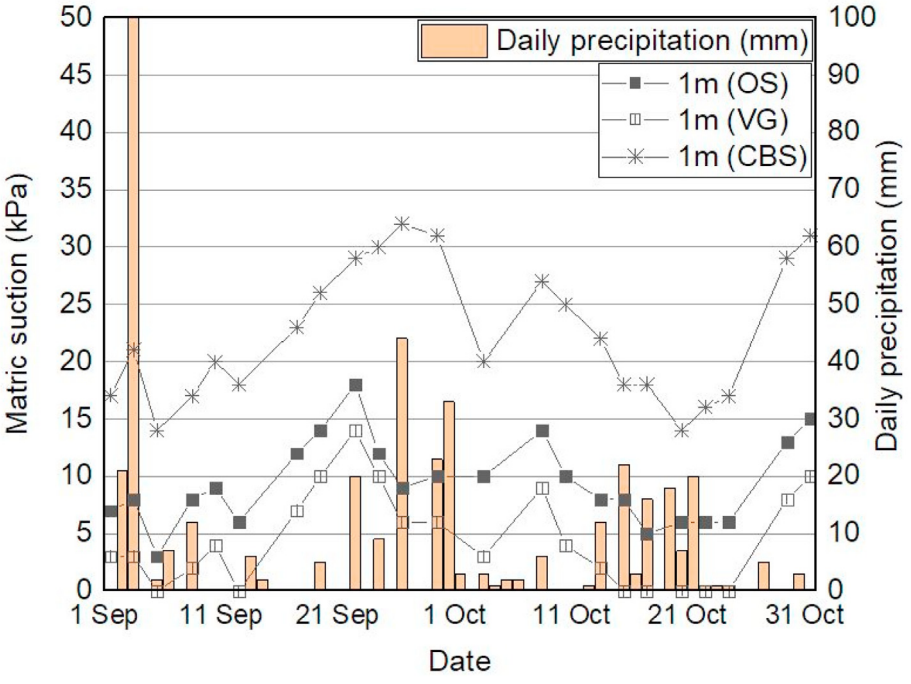

Fig. 13. Tensiometer measurements at 1 m depth for the original slope, vegetated slope and CBS slope.

analyses in the parametric studies. Based on the field measurements data, CBS was able to help increase the FOS of the slope by a maximum of 12% while Vetiver grass was able to help increase the FOS of the slope by a maximum of 8%. However, in the parametric studies, CBS was shown to help increase the FOS of the slope by a maximum of 25% while Vetiver grass helped to increase the FOS of the slope by a maximum of 4%. This could be attributed to the growth of roots of Vetiver grass with time that contributes matric suctions due to transpiration and therefore, the additional strength of the soil. This phenomenon could be captured from the instrumentation data, but it could not be reflected in the parametric studies.

4. Conclusions

The effect of CBS and Vetiver grass on slope stability was investigated through numerical analyses in terms of parametric studies and based on field measurements. The computed FOS from

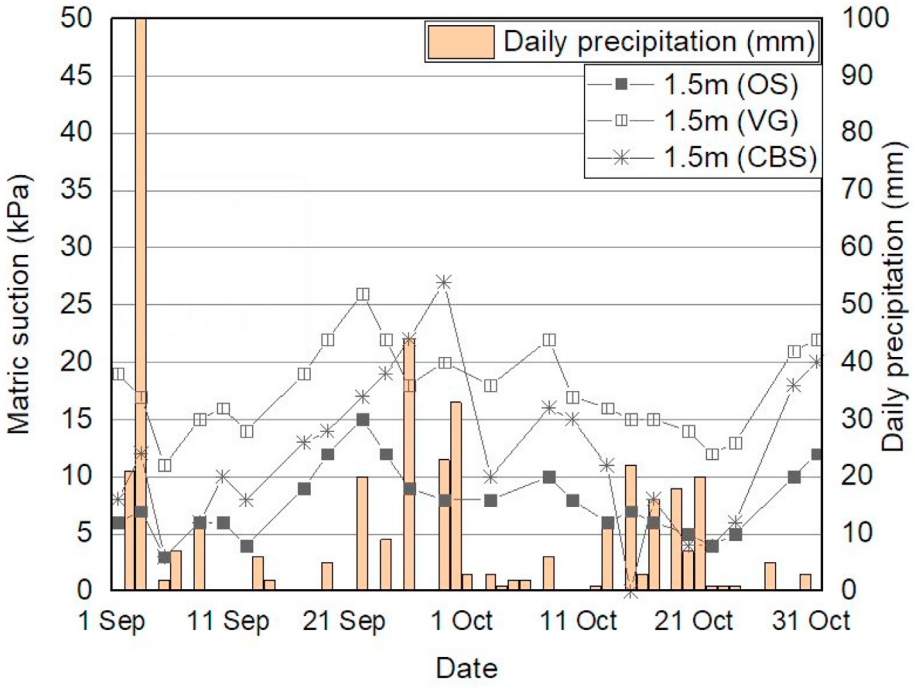

Fig. 14. Tensiometer measurements at 1.5 m depth for the original slope, vegetated slope and CBS slope.

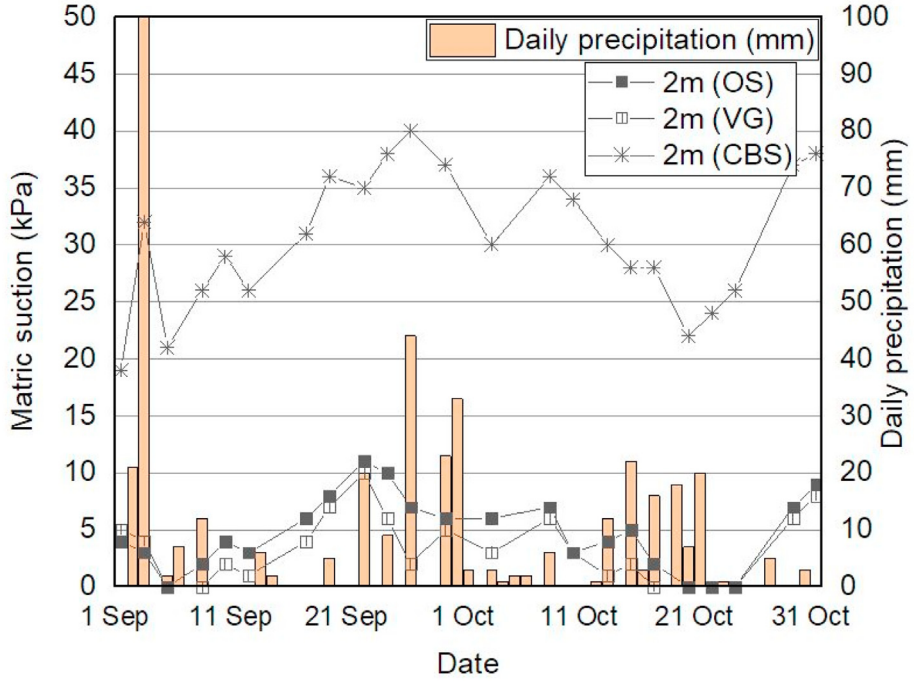

Fig. 15. Tensiometer measurements at 2 m depth for the original slope, vegetated slope and CBS slope.

numerical analyses results from the parametric studies and from the analyses by incorporating field measurements show that both CBS and Vetiver grass were able to stabilize slopes. However, it was observed that the CBS performed better than the vegetation in maintaining the stability of the slope in this study. It was also found that from the slope stability analyses in both parametric studies and field measurements, the CBS played a more effective role in limiting antecedent rainwater infiltration compared to the Vetiver grass, especially under the advanced and delayed rainfall patterns.

In future studies, it is recommended that the effect of vegetation growth on slope stability to be evaluated. The effect of vegetation growth on SWCC and permeability function of soil, as well as the evapotranspiration flux boundary can be incorporated in the seepage analyses. Moreover, the effect of vegetation growth on soil strength can be incorporated in the slope stability analyses.

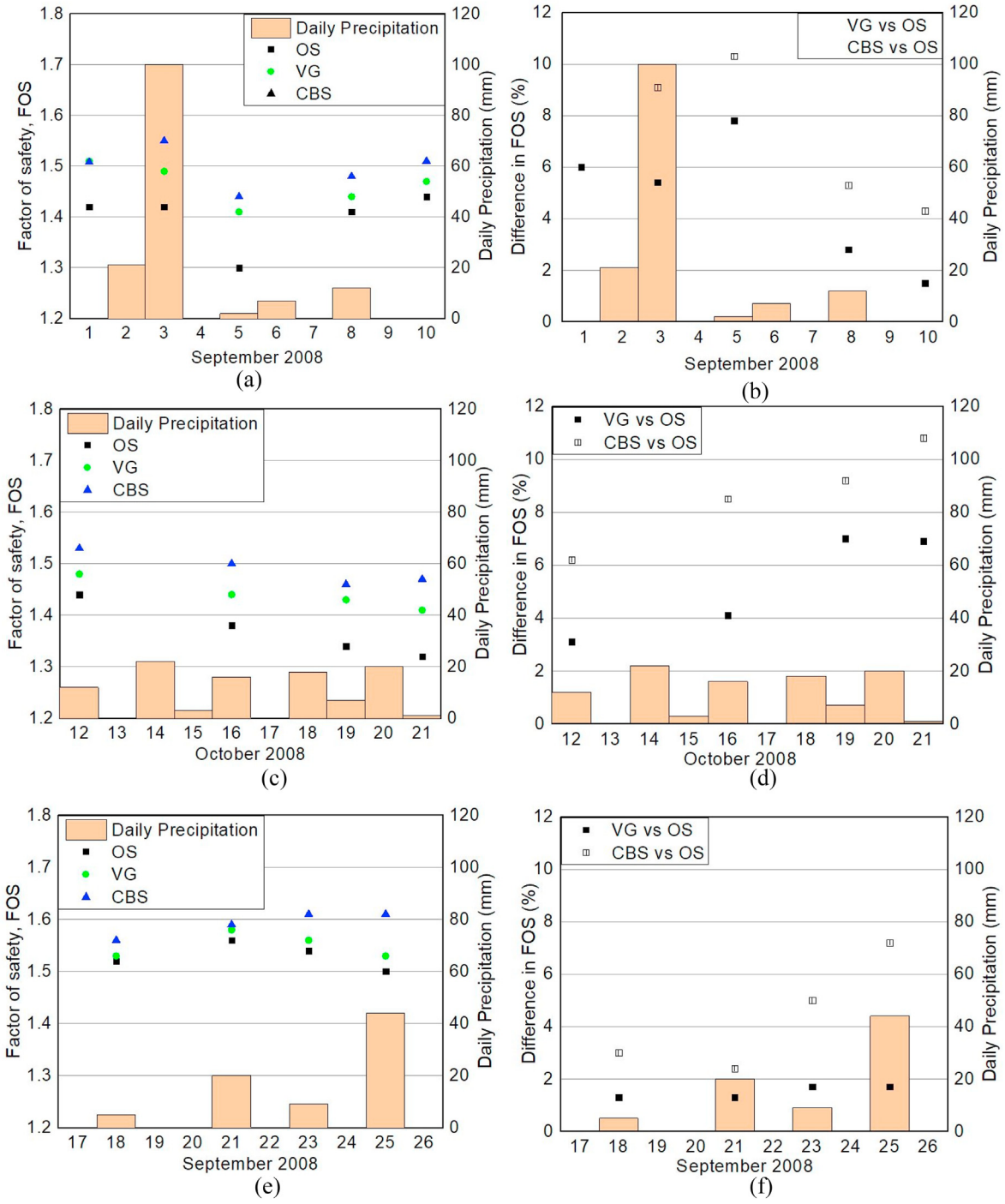

Fig. 16. The results of the FOS and difference in the FOS of the vegetated slope, CBS slope and original slope under the (a) (b) advanced rainfall pattern, (c) (d) normal rainfall pattern and (e) (f) delayed rainfall pattern.

Table 4
Comparison of effectiveness of CBS and Vetiver grass.

Max percentage of increase in the FOS compared to the original slope	Delayed rainfall pattern	Normal rainfall pattern	Advanced rainfall pattern
CBS (parametric studies)	25%	25%	20%
Vetiver Grass (parametric studies)	2.5%	4%	2.5%
Difference = CBS − Vetiver Grass (parametric studies)	22.5%	21%	17.5%
CBS (field)	7%	12%	11%
Vetiver Grass (field)	2%	7%	8%
Difference = CBS − Vetiver Grass (field)	5%	5%	3%

Declaration of competing interest

The authors declare that they have no known competing financial interests or personal relationships that could have appeared to influence the work reported in this paper.

Acknowledgement

This study was supported by the Housing and Development Board and Nanyang Technological University, Singapore.

References

Bishop, A. W. (1955). The use of the slip circle in the stability analysis of slopes. *Géotechnique, 5*(1), 7–17.
Brand, E. W., Premchitt, J., & Phillipson, H. B. (1984, September). Relationship between rainfall and landslides in Hong Kong. In *Proceedings of the 4th international symposium on landslides* (Vol. 1, pp. 377–384). Toronto: Canadian Geotechnical Society.
Comegna, L., Damiano, E., Greco, R., Guida, A., Olivares, L., & Picarelli, L. (2016). Field hydrological monitoring of a sloping shallow pyroclastic deposit. *Canadian Geotechnical Journal, 53*(7), 1125–1137.
Cuomo, S., Chareyre, B., d'Arista, P., Della Sala, M., & Cascini, L. (2016a). Micro-mechanical modelling of rainsplash erosion in unsaturated soils by Discrete Element Method. *Catena, 147*, 146–152.
Cuomo, S., & Della Sala, M. (2013). Rainfall-induced infiltration, runoff and failure in steep unsaturated shallow soil deposits. *Engineering Geology, 162*, 118–127.
Cuomo, S., Della Sala, M., & Novità, A. (2015). Physically based modelling of soil erosion induced by rainfall in small mountain basins. *Geomorphology, 243*, 106–115.
Cuomo, S., Della Sala, M., & Pierri, M. (2016b). Experimental evidences and numerical modelling of runoff and soil erosion in flume tests. *Catena, 147*, 61–70.
Forte, G., Pirone, M., Santo, A., Nicotera, M. V., & Urciuoli, G. (2019). Triggering and predisposing factors for flow-like landslides in pyroclastic soils: The case study of the lattari mts.(southern Italy). *Engineering Geology, 257*, Article 105137.
Fredlund, D. G., Morgenstern, N. R., & Widger, R. A. (1978). The shear strength of unsaturated soils. *Canadian Geotechnical Journal, 15*(3), 313–321.
Fredlund, D. G., & Rahardjo, H. (1993). *Soil mechanics for unsaturated soils*. John Wiley & Sons.
Fredlund, D. G., & Xing, A. (1994). Equations for the soil-water characteristic curve. *Canadian Geotechnical Journal, 31*(4), 521–532.
Fredlund, D. G., Xing, A., & Huang, S. (1994). Predicting the permeability function for unsaturated soils using the soil-water characteristic curve. *Canadian Geotechnical Journal, 31*(4), 533–546.
Geo-slope international Ltd. (2012a). *SEEP/W*. Calgary, Alberta, Canada: GEO-SLOPE International Ltd.
Geo-slope international Ltd. (2012b). *SLOPE/W*. Calgary, Alberta, Canada: GEO-SLOPE International Ltd.
Ghestem, M., Sidle, R. C., & Stokes, A. (2011). The influence of plant root systems on subsurface flow: Implications for slope stability. *BioScience, 61*(11), 869–879.
Greenwood, J. R., Norris, J. E., & Wint, J. (2004). Assessing the contribution of vegetation to slope stability. *Proceedings of the Institution of Civil Engineers-Geotechnical Engineering, 157*(4), 199–207.
Leong, E. C., & Rahardjo, H. (1997). Permeability functions for unsaturated soils. *Journal of Geotechnical and Geoenvironmental Engineering, 123*(12), 1118–1126.
Leung, A. K., Garg, A., & Ng, C. W. W. (2015). Effects of plant roots on soil-water retention and induced suction in vegetated soil. *Engineering Geology, 193*, 183–197.
Li, J. H., Du, L., Chen, R., & Zhang, L. M. (2013). Numerical investigation of the performance of covers with capillary barrier effects in South China. *Computers and Geotechnics, 48*, 304–315.
Meteorological Services Singapore. (2018). Past climate trends. http://www.weather.gov.sg/climate-past-climate-trends/.
Morris, C. E., & Stormont, J. C. (1999). Parametric study of unsaturated drainage layers in a capillary barrier. *Journal of Geotechnical and Geoenvironmental Engineering, 125*(12), 1057–1065.
Ng, C. W., Wang, B., & Tung, Y. K. (2001). Three-dimensional numerical investigations of groundwater responses in an unsaturated slope subjected to various rainfall patterns. *Canadian Geotechnical Journal, 38*(5), 1049–1062.
Ni, J. J., Leung, A. K., Ng, C. W. W., & Shao, W. (2018). Modelling hydro-mechanical reinforcements of plants to slope stability. *Computers and Geotechnics, 95*, 99–109.
Oh, S., & Lu, N. (2015). Slope stability analysis under unsaturated conditions: Case studies of rainfall-induced failure of cut slopes. *Engineering Geology, 184*, 96–103.
Pham, H. Q., Fredlund, D. G., & Barbour, S. L. (2005). A study of hysteresis models for soil-water characteristic curves. *Canadian Geotechnical Journal, 42*(6), 1548–1568.
Pirone, M., Papa, R., Nicotera, M. V., & Urciuoli, G. (2015). In situ monitoring of the groundwater field in an unsaturated pyroclastic slope for slope stability evaluation. *Landslides, 12*(2), 259–276.
Pradhan, A. M. S., & Kim, Y. T. (2015). Application and comparison of shallow landslide susceptibility models in weathered granite soil under extreme rainfall events. *Environmental Earth Sciences, 73*(9), 5761–5771.
Rahardjo, H., Leong, E. C., & Rezaur, R. B. (2008). Effect of antecedent rainfall on pore-water pressure distribution characteristics in residual soil slopes under tropical rainfall. *Hydrological Processes: International Journal, 22*(4), 506–523.
Rahardjo, H., Santoso, V. A., Leong, E. C., Ng, Y. S., & Hua, C. J. (2012). Performance of an instrumented slope covered by a capillary barrier system. *Journal of Geotechnical and Geoenvironmental Engineering, 138*(4), 481–490.
Rahardjo, H., Satyanaga, A., & Leong, E. C. (2013). Effects of flux boundary conditions on pore-water pressure distribution in slope. *Engineering Geology, 165*, 133–142.
Rahardjo, H., Satyanaga, A., Leong, E. C., Santoso, V. A., & Ng, Y. S. (2014). Performance of an instrumented slope covered with shrubs and deep-rooted grass. *Soils and Foundations, 54*(3), 417–425.
Rahimi, A., Rahardjo, H., & Leong, E. C. (2011). Effect of antecedent rainfall patterns on rainfall-induced slope failure. *Journal of Geotechnical and Geoenvironmental Engineering, 137*(5), 483–491.
Ross, B. (1990). The diversion capacity of capillary barriers. *Water Resources Research, 26*(10), 2625–2629.
Satyanaga, A., Rahardjo, H., & Hua, C. J. (2019). Numerical simulation of capillary barrier system under rainfall infiltration in Singapore. *ISSMGE International Journal of Geoengineering Case Histories, 5*(1), 43–54.
Schwarz, M., Preti, F., Giadrossich, F., Lehmann, P., & Or, D. (2010). Quantifying the role of vegetation in slope stability: A case study in tuscany (Italy). *Ecological Engineering, 36*(3), 285–291.
Sorbino, G., & Nicotera, M. V. (2013). Unsaturated soil mechanics in rainfall-induced flow landslides. *Engineering Geology, 165*, 105–132.
Stormont, J. C. (1996). The effectiveness of two capillary barriers on a 10% slope. *Geotechnical & Geological Engineering, 14*(4), 243–267.
Wang, K., Xu, Z. M., Tian, L., Ren, Z., Yang, K., Tang, Y. J., & Luo, J. Y. (2019). Estimating the dynamics of the groundwater in vegetated slopes based on the monitoring of streams. *Engineering Geology, 259*, Article 105160.
Xiong, X., Shi, Z., Xiong, Y., Peng, M., Ma, X., & Zhang, F. (2019). Unsaturated slope stability around the Three Gorges Reservoir under various combinations of rainfall and water level fluctuation. *Engineering Gceology, 261*, Article 105231.
Yan, C. G., Wan, Q., Xu, Y., Xie, Y., & Yin, P. (2018). Experimental study of barrier effect on moisture movement and mechanical behaviors of loess soil. *Engineering Geology, 240*, 1–9.
Zhai, Q., & Rahardjo, H. (2015). Estimation of permeability function from the soil–water characteristic curve. *Engineering Geology, 199*, 148–156.
Zhang, S., Zhang, X., Pei, X., Wang, S., Huang, R., Xu, Q., & Wang, Z. (2019). Model test study on the hydrological mechanisms and early warning thresholds for loess fill slope failure induced by rainfall. *Engineering Geology, 258*, Article 105135.